Atmos. Chem. Phys. Discuss., 11, 12849–12887, 2011
www.atmos-chem-phys-discuss.net/11/12849/2011/
doi:10.5194/acpd-11-12849-2011

Atmospheric Chemistry and Physics Discussions

Impact of a large wildfire on water-soluble organic aerosol in a major urban area: the 2009 Station Fire in Los Angeles County

A. Wonaschütz[1], S. P. Hersey[2], A. Sorooshian[1,3], J. S. Craven[2], A. R. Metcalf[2], R. C. Flagan[2], and J. H. Seinfeld[2]

[1]Department of Atmospheric Sciences, University of Arizona, P.O. Box 210081, Tucson, AZ 85721, USA
[2]Departments of Environmental Science and Engineering and Chemical Engineering, California Institute of Technology, 1200 E. California Blvd., Pasadena, CA 91125, USA
[3]Department of Chemical and Environmental Engineering, University of Arizona, P.O. Box 210011, Tucson, AZ 85721, USA

Received: 13 April 2011 – Accepted: 15 April 2011 – Published: 27 April 2011

Correspondence to: A. Sorooshian (armin@email.arizona.edu)

Published by Copernicus Publications on behalf of the European Geosciences Union.

Abstract

Water-soluble organic carbon is a major component of aerosol particles globally. This study examines a field dataset of water-soluble organic aerosol in the Los Angeles Basin, a classic urban setting, under typical conditions and under the influence of a large wildfire (the 2009 Station Fire). The measurements took place between July and September in Pasadena as part of the 2009 Pasadena Aerosol Characterization Observatory (PACO) field campaign. Large differences in the nature of water-soluble organic carbon (WSOC) were observed between periods with and without the influence of the fire. During non-fire periods, WSOC variability was driven most likely by a combination of photochemical production processes and subsequent sea breeze transport, resulting in an average diurnal cycle with a maximum at 15:00 LT (up to 4.9 µg C m^{-3}). During the Station Fire, smoke plumes advected to the site in the morning hours were characterized by high concentrations of WSOC (up to 41 µg C m^{-3}) in tight correlation with nitrate and chloride, and with Aerodyne Aerosol Mass Spectrometer (AMS) organic metrics such as the biomass burning tracer *m/z* 60, and total non-refractory organic mass. These concentrations and correlations and the proximity of the measurement site to the fire suggest that primary production was a key formation mechanism for WSOC. During the afternoons, the sea breeze transported urban pollution and processed residual smoke back to the measurement site, leading to higher afternoon WSOC levels than on non-fire days. Parameters representing higher degrees of oxidation of organics, including the ratios *m/z* 44 : *m/z* 57 and *m/z* 44 : *m/z* 43, were increased in those air masses. Intercomparisons of relative amounts of WSOC, AMS organic, *m/z* 44, and *m/z* 43 are used to examine how the relative abundance of different classes of WSOC species changed as a result of photochemical aging. The fraction of WSOC comprised of acid-oxygenates increased as a function of photochemical aging owing to the conversion of aliphatic and non-acid oxygenated organics to more acid-like organics. Assuming a factor of 1.8 to convert WSOC concentrations to organic mass-equivalent concentrations, the contribution of water-soluble organic

species to the organic mass budget (10th–90th percentile values) ranged between 27–72% and 27–68% during fire and non-fire periods, respectively. Therefore, WSOC is a significant contributor to the organic aerosol budget in this urban area. The influence of fires in this basin greatly enhances the importance of this class of organics, which has implications for the radiative and hygroscopic properties of the regional aerosol.

1 Introduction

Globally, roughly one half of atmospheric aerosol mass is organic, a fraction which can be even higher in urban areas. Typically between 40–85% of organic carbon measured in different locations worldwide has been shown to be water-soluble (Ruellan et al., 1999; Graham et al., 2002; Mayol-Bracero et al., 2002; Gao et al., 2003; Jaffrezo et al., 2005; Decesari et al., 2006). Water-soluble organic carbon (WSOC) species are emitted as primary particles, especially during biomass combustion, and produced as a result of reactions in the gas and aqueous phases (Miyazaki et al., 2006; Sullivan et al., 2006; Kondo et al., 2007; Weber et al., 2007; Ervens et al., 2010; Sorooshian et al., 2010; Timonen et al., 2010). Moreover, WSOC has been suggested as a marker for secondary organic aerosol (SOA) in the absence of biomass burning (e.g., Docherty et al., 2008).

The Los Angeles Basin has been the subject of many studies examining the transport and chemical evolution of atmospheric aerosols. Pasadena, the setting of this work, represents an area where particulate pollutant concentrations are governed by meteorology and numerous production and transport processes. The meteorology in the basin is characterized by early morning inversions, which, through increasing surface heating over the course of the morning, give way to a robust midday-afternoon sea breeze. Elevated pollution layers can form by horizontal and vertical displacement of the morning inversion layer and orographic uplift (Lu and Turco, 1995), allowing for aerosol processing in air masses separated from surface pollution sources during the day. These pollution layers can remain aloft during the night and re-entrain the next day through turbulent mixing in a deepening boundary layer, contributing to surface concentrations of aerosols (Husar et al., 1977; Blumenthal et al., 1978).

Organic compounds are a major constituent of the local pollution and are emitted directly as well as produced via secondary processes. Hughes et al. (2000) found increasing relative contributions of organic compounds to increasing mass concentrations of total suspended particulates and fine particles due to chemical processing along a sea breeze trajectory in the Los Angeles Basin. More recent measurements in the area during a normal summertime period showed that SOA is a major contributor to organic aerosol (Docherty et al., 2008), of which WSOC is an important component (Peltier et al., 2007). Owing to transport processes and spatial gradients in the oxidative capacity of the atmosphere, SOA is expected to contribute more to organic aerosol concentrations at inland areas than at the pollution source regions at the western side of the basin near the coast (Lu and Turco, 1995; Vutukuru et al., 2006).

In the late summer to fall months (August–November), following hot and dry summers, wildfires can be an additional component of the organic aerosol budget in the Los Angeles Basin (Phuleria et al., 2005). The Station Fire, which began on 26 August 2009 in the Angeles National Forest and came as close as 10 km to the PACO field site, was the tenth largest wildfire in modern California history and the largest ever in Los Angeles County, burning an area of more than 600 km^2 (California Department of Forestry and Fire Protection; http://bof.fire.ca.gov/incidents/incidents_archived). The impact of wildfires on urban aerosol physicochemical properties has been examined in other locations (Lee et al., 2008) but detailed aerosol studies examining the superposition of biomass burning emissions and typical Los Angeles atmospheric conditions are limited. The issue is especially of interest as wildfires in the Southwestern United States have been shown to have become more frequent and longer in duration compared to only a few decades ago and are expected to be a major concern in a future drier and warmer climate (Westerling et al., 2006).

An opportunity to study the nature of WSOC in the Los Angeles Basin in both the presence and absence of a major fire presented itself during the 2009 Pasadena

Aerosol Characterization Observatory (PACO) field campaign. The overall campaign is described in detail by Hersey et al. (2011). Here we report an analysis of the nature of particulate WSOC in Pasadena in a three-month period with an aim towards characterizing temporal concentrations, relative relationships with other organic aerosol metrics, sensitivity to meteorology and transport, and impact of the Station Fire. This work also provides a valuable database for comparison with subsequent field datasets collected from the surface and airborne platforms during the 2010 CalNex field campaign (http://www.esrl.noaa.gov/csd/calnex/).

2 Methods

2.1 Data

During the PACO field study (May–September 2009), ground-based measurements were conducted on the roof of the Keck Building on the campus of the California Institute of Technology (Caltech). The focus of this work is the period from 6 July 2009 to 16 September 2009. WSOC was measured in $PM_{2.5}$ every six minutes with a particle-into-liquid sampler (PILS; Brechtel Mfg. Inc.) coupled to a total organic carbon (TOC) analyzer (Sievers Model 800 Turbo, Boulder, CO). The instrument design and operational details are discussed extensively elsewhere (Sullivan et al., 2006). Briefly, particles smaller than 2.5 µm in diameter are sampled by the PILS and passed immediately through an organic carbon denuder (Sunset Laboratory Inc.) to remove organic vapors. Particles are then grown into droplets, which are collected by inertial impaction, and transported through a 0.5 µm PEEK (polyetheretherketone) liquid filter prior to entering a TOC analyzer for quantification of WSOC. A constant dilution factor of 1.15 is applied to account for dilution of the PILS liquid wash flow to the TOC analyzer owing to collected drops and condensation on the PILS droplet impactor. The reported WSOC levels are the difference between the measured and background concentrations. The overall measurement uncertainty is estimated to be approximately 10%.

Inorganic and non-refractory organic sub-micrometer aerosol measurements were carried out with an Aerodyne Compact Time of Flight Aerosol Mass Spectrometer (C-ToF-AMS) (Drewnick et al., 2005; Murphy et al., 2009) for the non-fire portion of the study and a High-Resolution AMS (HR-AMS) during the Station Fire. AMS data used here include organic markers at specific mass-to-charge ratios (*m/z*) that serve as proxies for organics with a range of oxidation states: acid-like oxygenated organics (*m/z* 44 = COO^+), aliphatic and non-acid oxygenated organics (*m/z* 43 = $C_3H_7^+$ and $C_2H_3O^+$; *m/z* 55 = $C_3H_3O^+$), aliphatic organics (*m/z* 57 = $C_4H_9^+$), and a biomass burning tracer (*m/z* 60) (McLafferty and Turecek, 1993; Zhang et al., 2005; Aiken et al., 2008; Ng et al., 2010; Alfarra et al., 2007). The PILS and AMS chemical measurements were time synchronized, accounting for sampling time delays in the PILS relative to the AMS (Sorooshian et al., 2006). The PILS sampled sub-2.5 µm particles while the AMS measured sub-micrometer particles; therefore, ratios of WSOC to AMS data represent an upper limit.

Particle size distribution measurements were carried out with a cylindrical scanning differential mobility analyzer (DMA; TSI Model 3081) coupled to a condensation particle counter (TSI Model 3760). Thirty-two days of hourly CO, O_3 and $PM_{2.5}$ measurements were obtained from ground sites in Pasadena (South Wilson Avenue), Upland, Burbank, and downtown Los Angeles (North Main Street) (http://www.arb.ca.gov) and are used to help interpret the WSOC data. Additional hourly meteorological data were obtained from the Mesowest database (http://mesowest.utah.edu/index.html). The stations used include the South Wilson Avenue station on the Caltech campus, the North Main Street station near downtown Los Angeles (∼ 12.5 km southwest of measurement site), and the Santa Fe Dam station ∼ 15 km east of the measurement site.

2.2 Fire development and influence on the measurement site

The Station Fire burned over several weeks. Its spatial extent and exact location, and thus the influence it exerted on the measurement site, changed over that time period. Figure 1 shows the progression of the fire over several days. The fire area was estimated from Moderate Resolution Imaging Spectroradiometer (MODIS) fire maps (http://firefly.geog.umd.edu/firemap/). The fire started on 26 August less than 10 km north of the sampling site and grew in areal extent over the next four days. It split into an eastern and a western part on 31 August. The western part quickly decreased in size while moving northward, was reduced to a relatively small remnant ~ 25 km northwest of the site by 2 September, and became unidentifiable by MODIS by 4 September. The eastern part remained sizeable, but moved farther eastward. Notable easterly wind patterns did not occur during the measurement period, making the eastern part of the fire an unlikely direct influence on the measurement site.

The dataset was split into a "fire period" and a "non-fire period" by examining the MODIS fire maps and using the AMS *m/z* 60 concentration as a tracer for biomass burning. The "fire period", consisting of the eight days between 26 August and 2 September, was marked by frequent high spikes in the measured *m/z* 60 concentration, reaching values up to 1.4 µg m^{-3}. The mean *m/z* 60 concentration over the fire period was 0.065 ± 0.122 µg m^{-3}. During the remaining measurement days ("non-fire period") the mean *m/z* 60 concentration was 0.013 ± 0.005 µg m^{-3}. While *m/z* 60 (and levoglucosan) have been shown to decay with exposure to the hydroxyl radical (Hennigan et al., 2010), the systematically higher levels of this mass spectral marker during the Station Fire make it a robust tool to identify periods with fire influence. CO similarly exhibited contrasting behavior during non-fire and fire periods, with mean concentrations of 0.13 ± 0.12 ppm$_v$ and 0.45 ± 0.50 ppm$_v$, respectively.

3 Results and discussion

3.1 PACO study background

Hersey et al. (2011) provide a comprehensive summary of the physical and chemical properties of aerosols sampled at the PACO measurement site over the time period between 10 July and 4 August, which overlaps with the beginning of the period examined

Title Page
Abstract | Introduction
Conclusions | References
Tables | Figures
◂| |▸
◂ ▸
Back | Close
Full Screen / Esc
Printer-friendly Version
Interactive Discussion

in this work. We briefly describe results from that study that are relevant to the interpretation of WSOC measurements during non-fire periods. Organic mass accounted for approximately 55% of the submicrometer AMS aerosol mass. Average organic carbon (OC) concentrations were greater by approximately 4% in the afternoons (15:00–19:00 LT) than in the mornings (07:00–11:00 LT). Conversely, elemental carbon (EC) decreased by approximately 22% from the mornings to the afternoons. Both trends lead to a much increased afternoon OC : EC ratio. It was concluded that production of primary organic carbon was relatively more important in the mornings while secondary production of organic carbon was more dominant in the afternoons. Size-resolved measurements showed that the afternoon submicrometer organic mass was bimodal with one modal vacuum aerodynamic diameter centered around 100–200 nm and another around 500–600 nm. Positive matrix factorization analysis showed that low-volatility and semi-volatile oxidized organic aerosol (LV-OOA and SV-OOA) accounted for 86% of organic aerosol, suggestive of a large contribution by an oxidized organic fraction. The following sections will examine the nature and character of the WSOC fraction of the aerosol, which coincides with this highly oxidized organic fraction.

3.2 Meteorological setting and origin of air masses

Weather conditions were warm and dry during the entire WSOC measurement period (Fig. 2). Ambient temperatures ranged from 15° to ~ 40 °C. Relative humidity (RH) usually dropped below 40% during the day but reached 100% in the early morning hours of many days. Temperatures averaged several degrees higher during the Station Fire period, while RH was around 20% lower, helping to sustain the duration and spread of the fire. Air mass back-trajectories calculated with the NOAA HYSPLIT model (Draxler and Rolph, 2003) showed that sampled air masses were generally of marine origin with brief continental exposure prior to reaching the sampling site.

As the western edge of the Los Angeles Basin is major source region for pollutants (Lu and Turco, 1995), it is important to identify dominant wind patterns and transport times to Pasadena. Figure 3 shows the local wind characteristics at South Wilson

Avenue/Caltech Campus and at several surrounding stations. The most common wind directions at all stations are southerly to westerly, a manifestation of the sea breeze. The diurnal development of wind at South Wilson Avenue starts with very calm air at night and in the early mornings. During the late morning hours the wind tends to turn clockwise from the NE through S to the predominant afternoon sea breeze direction from the SW. Wind speeds increase during the development of the sea breeze in the afternoons. Initially stagnant air in the early morning is therefore, over the course of the late morning, expected to be influenced by air masses from more polluted urban areas and ultimately replaced by air masses of largely marine origin with anthropogenic influence, carrying particles with a mix of fresh and aged components. In the mornings, the air is expected to be more influenced by local sources, as well as by accumulated residual pollution from the previous day. The South Wilson Avenue Station measures systematically lower wind speeds than the surrounding stations, which is likely a localized effect caused by buildings and trees in the immediate surroundings of the site. Wind speeds measured at that site are therefore assumed to represent a lower limit of the areal wind speed. A statistical analysis of wind speeds and directions between 13:00–18:00 LT showed that the most common wind speeds were 4.5 m s^{-1} at North Main Street and 1.3 m s^{-1} at South Wilson Avenue. The most common wind directions were 270° and 225°, respectively. The afternoon transport time of urban pollution from downtown Los Angeles to Pasadena is thus on the order of 1–2 h (13:00–18:00 LT), consistent with the estimate by Hersey et al. (2011) for the period between May and August 2009. Given the most common afternoon wind speed at North Main Street, the transport time of anthropogenically influenced marine air from the coast to Pasadena from a southwesterly direction is approximately two hours.

3.3 WSOC production pathways and relationship with ozone

Identifying the relative importance of primary and secondary production mechanisms of WSOC is difficult given diurnal complexities in aerosol and precursor emissions, transport patterns and dynamic vertical structure of the boundary layer in the basin

(Blumenthal et al., 1978; Vutukuru et al., 2006). WSOC concentrations measured on non-fire days may be governed by all or a subset of the following mechanisms: 1. local primary production of WSOC; 2. local secondary production; 3. advection of existing WSOC that was either primarily or secondarily produced; 4. advection of precursor VOCs, with WSOC production occurring during transport; 5. volatilization and subsequent oxidation into SOA of semivolatile primary organic aerosol (POA) (Robinson et al., 2007); and 6. re-entrainment of pollution layers aloft. The Station Fire adds another level of complexity as additional sources of WSOC include direct emission of WSOC and secondary production from precursors emitted in the fire.

Previous work in the study region has shown that the temporal behavior of organic aerosol is closely related to that of O_3, indicative of photochemical production of SOA (Hersey et al., 2011). In Pasadena, WSOC peaks after O_3 on 16 out of 20 examined days with a typical time lag of 1.5–2.5 h. WSOC peaks occurred simultaneously or slightly before O_3 peaks (0.5 h) on 3 days, and only on one day did the WSOC peak precede an unusually late O_3 peak by hours. This points to a strong link between overall WSOC concentrations and photochemical processes.

The variability of O_3 concentrations at different ground sites in the Los Angeles basin provides insight into the spatiotemporal behavior of photochemical processes and the photochemical potential at the Pasadena site. O_3 concentrations measured at ground stations in Pasadena (South Wilson Avenue), Burbank, Upland and downtown Los Angeles (North Main Street) were examined for a period of 24 days in July (a subset of those days is shown in Fig. 7). In the prevailing sea breeze regime, transport of precursors from downtown Los Angeles (a classic pollutant source location) is expected to influence O_3 concentrations at the measurement site. On 10 out of the examined 24 non-fire days, O_3 peaked in downtown Los Angeles approximately an hour before it did in Pasadena, consistent with the transport times of 1–2 h given most common mid-afternoon (13:00 to 16:00 LT) wind speeds of 1.3 $\mathrm{m\,s^{-1}}$ in Pasadena and 3.6 $\mathrm{m\,s^{-1}}$ at downtown Los Angeles. Peak O_3 concentrations in Pasadena were consistently higher (22 out of 24 days) than in downtown Los Angeles, owing to additional time for photochemical processing of O_3 precursors in addition to the expected advection of O_3 itself from upwind locations. The farther downwind site of Upland is characterized by even higher and more delayed O_3 peaks. This observed spatial O_3 behavior and its implications for SOA production are consistent with the findings of Vutukuru et al. (2006) who showed that SOA levels in the basin are higher at inland (e.g., Azusa, Riverside) than at coastal sites. However, on six days (two of which are discussed in the case study below) O_3 reached peak concentrations in Pasadena before it did so in downtown Los Angeles (an average of 1.5 h earlier) and on six other days (one of which is discussed in the case study below), it peaked within the same hour as in downtown Los Angeles. These days were not associated with unusual wind directions or increased wind speeds. Local sources, downward mixing of elevated pollution layers from previous days in a deepening mixed layer, and/or unusually vigorous photochemical activity (as described by Hersey et al., 2011) could explain these "early" O_3 peaks. Therefore, advection of oxidants from downtown Los Angeles on any given day is not necessarily a requirement for photochemical activity in Pasadena.

3.4 Cumulative WSOC statistics

During the non-fire period, the highest WSOC concentration measured was 4.9 µg C m^{-3}. The observed concentration range is consistent with that of independent measurements in other urban areas (Jaffrezo et al., 2005; Sullivan et al., 2004, 2006; Kondo et al., 2007), including those in nearby Riverside during the summer of 2005 (Peltier et al., 2007). WSOC exhibits a weak correlation with solar radiation ($r^2 = 0.28$) and somewhat higher correlations with O_3 ($r^2 = 0.35$) and T ($r^2 = 0.44$) (Table 1). The low correlations with meteorological parameters are likely due to the complexity of the processes governing WSOC levels in Pasadena, including diverse sources, and the superposition of secondary formation and transport processes. The highest correlations between WSOC and AMS aerosol components were found for the following organic markers: *m/z* 43 ($r^2 = 0.49$), total AMS organic mass ($r^2 = 0.47$), and *m/z* 55 and 60 ($r^2 = 0.45$). Although *m/z* 55 and *m/z* 43 are prominent components in traffic emissions, they are more related to oxygenated organics than the primary hydrocarbon-like organic aerosol (HOA) marker *m/z* 57 (e.g., Zhang et al., 2005); for example, they are less correlated with NO_x and CO. As a result, the correlation of WSOC with *m/z* 57 ($r^2 = 0.20$) is the lowest among the correlations with AMS organic markers. WSOC exhibits little to no correlation with the inorganic compounds nitrate (NO_3^-), sulfate (SO_4^{2-}), chloride (Cl^-), and ammonium (NH_4^+) ($r^2 \leq 0.08$).

During the fire period, the range of measured WSOC levels (0.8–40.6 µg C m^{-3}) was consistent with that observed in other measurements with major biomass burning influences: 11–46 µg C m^{-3} (Mayol-Bracero et al., 2002), 2.2–39.6 µg C m^{-3} (Graham et al., 2002), 4.4–52.6 µg C m^{-3} (Decesari et al., 2006), and 0.57–18.45 µg C m^{-3} (Sullivan et al., 2006). The highest WSOC concentration, 40.6 µg C m^{-3}, was measured in the morning of 30 August. WSOC correlations (r^2) with most organic metrics (i.e. total AMS organic mass and *m/z* 44, 60, 43, and 55, but not *m/z* 57) ranged between 0.80 and 0.92 (cf. 0.35 and 0.49 during non-fire periods). The systematically higher correlations during the fire period indicate that there likely was a single dominating factor governing the variability of both organic and WSOC levels; since WSOC was highly correlated with *m/z* 60 ($r^2 = 0.90$), fire emissions were clearly influential. A high correlation between WSOC and NO_3^- was observed ($r^2 = 0.79$), followed by WSOC and Cl^- ($r^2 = 0.57$), but correlations with NH_4^+ and SO_4^{2-} ($r^2 \leq 0.18$) were poor. Fresh biomass burning emissions consist mainly of organic carbonaceous components and have been reported to have only minor contributions from inorganic species (Reid et al., 2005; Fuzzi et al., 2007; Grieshop et al., 2009); however, enhanced NO_3^- concentrations have been observed in smoke plumes (Gao et al., 2003; Reid et al., 2005; Peltier et al., 2007). Potassium chloride is also thought to be a common constituent in fire emissions (Posfai et al., 2003; Reid et al., 2005), which can explain the enhanced correlation of WSOC and Cl^-, providing additional support for a primary production mechanism. The correlation of WSOC with O_3 is absent during the fire period, even though O_3 concentrations are influenced by the fire (peak concentrations in the diurnal average of 91.5 ppb_v during the fire vs. 58.5 ppb_v for the non-fire diurnal average;

Fig. 2). This also indicates that photochemical production is not the dominant process governing the large increases of WSOC concentrations during the fire.

During the fire period, the ratio of WSOC to organic mass ranged from 0.11 to 0.53 µg C/µg, with a 10th percentile of 0.15 and a 90th percentile of 0.40. After converting the 10th and 90th percentile values to an equivalent organic mass concentration using a factor of 1.8 (Docherty et al., 2008), water soluble organics are estimated to account for between 27% and 72% (with an average of 47 ± 15%) of the organic mass. The WSOC : organic ratio range during the non-fire period is similar (10th/90th = 0.15/0.38), which after applying the 1.8 conversion factor to WSOC results in a 10th–90th percentile range of 27–68% (average = 45 ± 16%).

3.5 Diurnal WSOC behavior

During the non-fire period, the daytime diurnal average concentration of WSOC (Fig. 4) exhibits a maximum around 15:00 LT, coincident with maxima in AMS organic mass, *m/z* 44 and 43, but after O_3 (13:00) and solar radiation (14:00) (Fig. 2). Since wind direction itself has a pronounced diurnal cycle, the afternoon peak in WSOC can be plausibly explained by both photochemical production and/or transport from downtown Los Angeles via the afternoon sea breeze (a complication in explaining diurnal variability of pollutants noted specifically for Pasadena by Blumenthal et al., 1978). The behavior of *m/z* 57 provides some insight: while it does show an increase starting at 06:00 and a local peak at 09:00, consistent with local rush hour traffic (confirmed with ground-based CO data, Fig. 8), its maximum concentration occurs at 13:00, when local primary emissions are expected to be lower than in the morning. Since all organic metrics including *m/z* 57 reach their highest concentrations with high temporal coincidence in the early afternoon, it is likely that transport from more polluted areas, including downtown Los Angeles, plays a major role. While the contribution of organics to total AMS mass increases from 06:00 to 15:00, WSOC : organic is relatively constant until it begins to increase at 14:00 (Fig. 5). The majority of the relative increase of WSOC to organics occurs between 14:00–19:30, during a decrease of total AMS mass, WSOC, and organic m/z markers shown (Fig. 4). The advancing sea breeze front is known to produce strong gradients in secondary pollutants (Lu and Turco, 1995). Thus, a likely scenario for the relative increase of WSOC during the decrease of absolute concentrations of most every organic marker is the superposition of secondary production of WSOC by photochemical processing and transport of cleaner and more aged marine air to the site. The ratio m/z 44:57 increases with WSOC:organic, indicative of an increasing oxidized fraction of the organic aerosol.

During the fire period, organics dominated the sub-micrometer aerosol mass, with significantly higher organic mass fractions than in the non-fire period (Fig. 5). The contribution of WSOC to organics was systematically elevated from the early morning hours through the late afternoon, with relatively stable and higher ratios between 04:00–12:00 compared to other times. WSOC concentrations peaked in the mornings. Average WSOC concentrations (Fig. 4) were higher by a factor of 10 than in the non-fire period at ~08:30. Lower wind speeds during the mornings promoted accumulation of smoke, and variable wind directions allowed for smoke from the burning areas to be advected to the sampling site and farther into the basin. The diurnal behavior of the biomass burning tracer m/z 60 matches that of WSOC (with the exception of a sharper decrease from 08:00 to 12:00), providing evidence for the presence of biomass burning aerosols at the measurement site when WSOC increased in concentration. In the afternoon, southwesterly winds directed smoke plumes away from the measurement site, leading to a decrease in measured WSOC concentrations. The afternoon peak of diurnally-averaged WSOC at 15:00 that was evident during the non-fire period is barely visible given the high WSOC concentrations during earlier parts of the days; nonetheless, the diurnal average WSOC concentration at this time of day exceeds that of the non-fire period by a factor of 1.5. As organic precursors emitted in the fire were likely present in the entire Los Angeles basin after several days of burning, residual and processed smoke are thought to have played an additional role in the usual transport of pollutants by the afternoon sea breeze. The fire period exhibits an earlier rise and higher maximum of the diurnal average O_3 concentrations than the non-fire period, underlining the impact of the fire on the timing and magnitude of photochemical activity. There are large systematic increases in the *m/z* 44 : 43 and *m/z* 44 : 57 ratios between 09:00–15:00 during the fire (Fig. 5), at times when the absolute values of all organic measurements decreased after the major morning peaks (cf. Fig. 4). The larger absolute increases of these ratios in the fire compared to non-fire conditions points to a more vigorous conversion of organics towards a more oxidized state at a relatively stable WSOC : organic ratio.

3.6 Relationships between WSOC, AMS organic, *m/z* 44, and *m/z* 43

Since WSOC comprises both hydrophobic and hydrophilic fractions (e.g., Sullivan and Weber, 2006), it is of interest to examine the relative behavior of *m/z* 44, *m/z* 43, total AMS organic, and WSOC. Given that the fire constitutes a source of WSOC that is very different from those that are dominant during non-fire days, the chemical nature of the WSOC measured in the morning smoke-plumes is expected to differ from that measured in the afternoons. Morning-to-afternoon ratios (i.e. concentrations at 08:00 LT vs. 14:00 LT) of diurnally-averaged *m/z* 44, 43, 60, organic, and WSOC concentrations (shown in Fig. 4) are examined to explore these potential differences. The smallest morning-to-afternoon ratio for any of these organic metrics was for *m/z* 44 (1.9), followed by AMS organic (2.4), *m/z* 43 (2.7), and WSOC (3.3). The morning-to-afternoon ratio for *m/z* 60 was 9.6, confirming the much larger direct influence of the fire in the morning. Given the different morning-to-afternoon ratios of *m/z* 44 and 43, it is plausible that the afternoon WSOC contained constituents produced as a result of photochemical processing of smoke, with more of the non-acid oxygenates having been converted to acid-like oxygenates.

Recent studies have utilized *m/z* 44 and *m/z* 43 (Ng et al., 2010; Chhabra et al., 2011) to track the aging of organic aerosols in the atmosphere. Hersey et al. (2011) conducted an analysis of f_{44} (*m/z* 44 : total organic signal) vs. f_{43} (*m/z* 43 : total organic signal) for Los Angeles aerosol, where higher levels of f_{44} relative to f_{43} are thought to indicate a greater degree of organic oxygenation and lower volatility. They observed a high level of consistency in the overall degree of oxidation of the aerosol over a span of several months between May and August of 2009. Ng et al. (2010) suggested an alternative way to conduct a similar type of analysis that can incorporate measurements from instruments other than the AMS (see their Fig. 5). They specifically used multiple field datasets to plot f_{44} and the O : C ratio vs. m/z 44 : 43 and observed that both f_{44} and the O : C ratio increase sharply at the beginning of oxidation and then plateau at larger m/z 44 : 43 ratios, suggesting the existence of a maximum oxidation state of the aerosol. Figure 6 examines the ratios of m/z 44 : WSOC and WSOC : organic as functions of the m/z 44 : 43 ratio for both the fire- and non-fire period. The m/z 44 : 43 ratios range between 0.6–2.7 (non-fire period) and 1.1–3.1 (fire period). In the mentioned plot in Ng et al. (2010, Fig. 5), this is a range in which the O : C ratio and f_{44} are increasing rapidly prior to reaching a plateau. We first note that the product of the quantities displayed on the y-axes in Fig. 6 (m/z 44 : WSOC × WSOC : organic) is equivalent to f_{44}, which when examined as a function of m/z 44 : 43 qualitatively reproduces the curve shown in Ng et al. (2010). During both the fire-and non-fire period, the m/z 44 : WSOC ratio grows as a function of m/z 44 : 43, indicating that the contribution of acid-like oxygenates to WSOC increases as the chemical functionality of the species contributing to m/z 44 and 43 move towards a more oxidized state. This is most clearly illustrated by the data representing the greatest influence by the smoke plume (larger symbols in Fig. 6). The early morning fire plumes advected to the measurement site exhibit relatively low values of m/z 44 : 43. The m/z 44 : WSOC ratio increased gradually as a function of m/z 44 : 43 and time of day, suggesting that conditions associated with transitioning from morning to afternoon hours (higher temperatures, O_3, solar radiation, changing wind direction) promoted processing of organics to contain more oxidized organics and transport of these processed species back to the sampling site. The WSOC : organic ratio is a less variable function of m/z 44 : 43 than the m/z 44 : WSOC ratio. This is because WSOC consists of species including those represented by m/z 44 and 43. Changes in the chemical functionality of m/z 44 and 43 are thus not necessarily expected to cause variability of WSOC : organic. WSOC : organic ratios most influenced by the fire plume (larger symbols in Fig. 6) have a relatively constant value across the observed range of *m/z* 44 : 43, suggesting that the more noticeable effect of photochemical processing during the day was to transform components of the WSOC into more oxidized forms rather than to produce more WSOC mass.

3.7 Case studies

3.7.1 Non-fire period (7 July 2009–15 July 2009)

A period of five days between 7 July 2009 and 15 July 2009 is used to study the nature of WSOC during non-fire days more closely (Fig. 8). Ground station data for CO, O_3, and $PM_{2.5}$ across the Los Angeles basin for this time period are shown in Fig. 7. WSOC concentrations always peaked between 13:00–14:00 LT and usually did so immediately after or simultaneously with O_3. The range of absolute WSOC concentrations was similar from day to day, but there were large differences in the temporal concentration profiles. CO levels were usually lower in Pasadena than at the other sites, indicative of a less pronounced influence of local traffic emissions.

On 7 July (Tuesday), the wind in Pasadena was low from the NW to NE until 10:00, and then increased gradually while turning to a southerly direction. The sea breeze was fully developed by noon. There was remarkable covariance between WSOC, AMS organic, numerous *m/z* markers (43, 44, 55, 57, 60), and the ratio of WSOC : total AMS mass. Their common behavior features a smooth morning increase followed by an equally smooth afternoon decrease. The WSOC concentration increased from 0.96 µg C m^{-3} at 07:30 to 3.41 µg C m^{-3} at 14:00 before gradually decreasing to 1.44 µg C m^{-3} at 19:00. The ratio of WSOC : organic, which would be expected to increase during photochemical WSOC production, remained relatively stable through the entire day. Transport of pollution was a major factor in influencing the observed increase in WSOC concentration; however, this does not preclude the possibility that the measured WSOC in Pasadena was secondarily produced upwind or during transport. Hersey et al. (2011) noted that semi-volatile OOA (SV-OOA) was well correlated with O_3 and associated with peaks in DMA number concentration, suggestive of early generation SOA products that are 1–2 h old. This is consistent with our observations on 7 July: a number of metrics for the degree of organic oxidation (e.g. *m/z* 44 : 43 and *m/z* 44 : 57) began to decrease starting around 11:00–12:00, while O_3 concentrations increased and the sea breeze advected fresh and processed organics to the measurement site. AMS inorganic species did not follow the behavior of the organic species. The afternoon increase in SO_4^{2-} coupled with the decrease of organics can be attributed to the increasing wind speed and influx of marine air.

The importance of wind direction is illustrated on 10 July 2009 (Friday) as WSOC sharply declined in concentration (from 2.05 to 0.48 µg C m^{-3} between 11:40–13:20) and then increased to 3.93 µg C m^{-3} between 14:00 and 16:00. This behavior is qualitatively reflected in all other parameters shown in Fig. 8 (with the exception of O_3) and is also visible in the size distribution data as a sudden decrease in both number and volume concentrations over all particle sizes (Fig. 9). In the time period of lower concentrations, the wind, previously from S to SE, shifted to a northeasterly direction at a speed of 1.3 m s^{-1}, carrying in a less polluted air mass with lower WSOC concentrations. O_3 concentrations were not impacted by the wind shift, but exhibited a typical smooth diurnal cycle consisting of a gradual increase up to a peak concentration at 14:00, followed by a decrease for the rest of the day. This mismatch between WSOC and O_3 concentration changes indicates that transport rather than local photochemical production dominated WSOC variability in the earlier part of this day. The wind shifted to a southwesterly direction between 14:00 and 16:00, leading to initially increasing WSOC levels and DMA number concentrations, which then decreased due to continuing sea breeze winds and a decrease in photooxidation corresponding to decreased intensity of solar radiation. Similar trends between WSOC and DMA size distribution data were observed on 11 July 2009.

During the last two days of this case study period (Tuesday and Wednesday; 14 and 15 July), the peak WSOC concentration did not lag as far behind maximum O_3 levels as on previous days. Furthermore, on 15 July, WSOC concentrations began to increase in the afternoon before the sea breeze was fully established, indicating that local photochemical production may have played a somewhat more important role than on the other case study days. Later in the day, the advection of cleaner air by the sea breeze reduced concentrations of WSOC and AMS organic species. Thus, photochemical processes are important for overall WSOC production in the basin, but much of the measured variability of WSOC in Pasadena is dominated by transport effects.

3.7.2 Station fire period (27 August 2009–2 September 2009)

While diurnal average features of the fire days have been discussed, more details about day-to-day variability and daily features of aerosol parameters over a period of seven successive days are shown in Fig. 10, with associated basin-wide gas and $PM_{2.5}$ ground station data shown in Fig. 7. The impact of the fire on the sampling site was variable, ranging from large increases of every measured quantity on 28, 30 and 31 August, to much lower impacts on 29 August and 1 September. In Fig. 10, the connection between wind and smoke influence on aerosol composition is clearly visible: using *m/z* 60 as a tracer for the smoke plume, it is evident that periods with low wind speeds and wind directions with a northerly component feature the highest smoke concentrations. The fact that measured concentrations of *m/z* 60 were higher in the morning hours than in the evenings (when wind speeds are equally low) may be due to the boundary layer being most shallow and stagnant conditions having persisted for a number of hours by the morning. On individual days, the dynamic development of the fire itself may play a role as well. Concentrations of *m/z* 60 decrease immediately as the wind direction shifts and the wind speed picks up in the developing sea breeze.

The ground station data (Fig. 7) reflect the impact of the fire on the entire Los Angeles basin: CO, a tracer for combustion processes, reaches its highest values on the mornings of 30 and 31 August, especially in Pasadena and Burbank which, of the four sites, were the closest to the fire. During the nine non-fire days, typical rush hour $PM_{2.5}$ levels in downtown LA ranged from 30 to 50 $\mu g\,m^{-3}$, whereas on 30 and

31 August, they reached 149 and 73 µg m^{-3}, respectively, showing that the fire had a direct influence on locations farther south and southwest of Pasadena. Thus, even when the afternoon sea breeze directed the smoke plume away from the site, it still transported aged smoke to the site. O_3 exhibited systematically higher levels at all four stations, especially on 30 and 31 August.

The mornings of 28, 30 and 31 August are particularly impacted by the accumulation of smoke. WSOC shows a very tight correlation with *m/z* 60, NO_3^-, and Cl^- during the smoke events. Most other organic metrics also vary in lockstep with WSOC with the notable exception of SO_4^{2-}, which exhibited a poor correlation with WSOC and lower levels in the diurnal average than on non-fire days. Reid et al. (2005) note that while SO_4^{2-} is a secondary product of biomass burning, its production requires high relative humidity, a requirement which was not met during the PACO fire period. Given this lack of liquid-phase SO_4^{2-} production, and the low relative humidity observed during the majority of the study period, it is unlikely that liquid-phase processes played a key role in WSOC production (e.g., Hennigan et al., 2008, 2009) during either the fire or the non-fire period. In the afternoons of 28, 30 and 31 August, the temporal behavior of WSOC, *m/z* 60, and AMS organic metric concentrations became less coordinated. While the developing sea breeze started to direct the smoke away from the site, the residual smoke was subject to photochemical processing, as indicated by the rise in *m/z* 44 : 57 and *m/z* 44 : 43 and the unusually high O_3 concentrations (176 ppb$_v$ at 14:00 on 30 August and 124 ppb$_v$ at 10:00 on 31 August). Afternoon WSOC concentrations were about a factor of two higher than the non-fire average. Concentrations of *m/z* 60 were elevated by a factor of two to three above average non-fire concentrations, which is expected given that smoke at that point would have distributed all over the basin, as confirmed by the observed smoke influence in downtown Los Angeles (Fig. 7). On 27 and 29 August, the spectacular morning smoke plumes observed on the days discussed above were absent; however, both O_3 and afternoon WSOC concentrations are above the non-fire average (WSOC: 3.8 µg m^{-3} at 15:10 on 29 August and 11.2 µg m^{-3} at 11:50 on 27 August), reflecting contributions of transported aerosols in the sea breeze containing aged smoke and fresh and processed anthropogenic aerosols.

Figure 9 shows the development of sub-micrometer number and volume size distributions on 31 August, a day with significant fire influence. It is evident that the smoke event between 02:00 and 12:00 LT is associated with larger particles (modal diameter of about 150 nm) than typically observed during that time on non-fire days (modal diameter of 80 nm) and that most of the volume is concentrated around 230 nm. At 12:00, there was a distinct shift to smaller particles (around 40 nm), which coincided with a decrease in WSOC concentrations (Fig. 10). The concentration of these smaller particles subsequently increased and reached a maximum at approximately 15:00, coinciding with an increase in WSOC concentrations owing most likely to photochemical production.

4 Conclusions

This work examines a ground-based field dataset of WSOC in conjunction with numerous other aerosol, gas, and meteorological measurements. Two periods governed by the presence and absence of a major wildfire are separately examined with respect to WSOC and the processes governing its temporal variability at a fixed site in Pasadena, California. WSOC is considered a tracer for SOA in the absence of biomass burning due to its highly oxidized nature. The PACO study showed that in the absence of biomass burning, changes in WSOC concentrations in Pasadena are largely driven by the diurnal sea breeze circulation and concurrent photooxidation of the transported airmasses. Initially, in the early afternoon, the sea breeze transports pollutants from the direction of the source-rich downtown Los Angeles area to Pasadena. Chemical processing of those air masses likely occurs while they are on their way and contributes to the temporal WSOC concentration gradient observed at the measurement site, in addition to the influx of WSOC that was already produced at upwind locations. Later in the afternoons, the continuing sea breeze brings in cleaner air masses while photochemical activity decreases with reduced intensity of solar radiation. These processes cause a marked decrease in WSOC, but enhanced WSOC : organic ratios. Given our observations, photochemical processes are important for overall WSOC formation in the Los Angeles basin, but cannot be assumed to dominate the observed variability at a single site. That variability is determined by a combination of transport and secondary formation processes, as well as factors we were unable to quantify, such as the magnitude of residual WSOC levels in upwind areas and in layers aloft that may be mixed into the boundary layer as a result of surface heating and boundary layer deepening over the course of the day.

During the Station Fire, WSOC concentrations and their contributions to total organic mass were significantly higher than on typical non-fire days. WSOC was produced via both primary and secondary pathways. Close covariance of WSOC with many other measured species (nitrate, chloride, total AMS organic aerosol mass) in smoke events (defined by unusually high *m/z* 60 concentrations in stagnant/northerly wind conditions) is a good indicator for primary (and potentially sufficiently fast secondary) production of WSOC in the fire emissions. Secondary production of WSOC becomes detectable after the initial morning smoke plumes are directed away from the sampling site and aged smoke from farther upwind makes its way back to the measurement site with the afternoon sea breeze. Increasing *m/z* 44 : 57 and *m/z* 44 : 43 ratios show the ongoing oxidation of the smoke-influenced air masses once they arrive back at the measurement site with the sea breeze. Unusually high and early O_3 concentration maxima indicate high photochemical activity, which may also lead to some of the increased WSOC concentrations observed outside of the direct smoke plume. Multiphase processes were not a significant source of WSOC owing to low relative humidities during the entire study.

A close examination of the relationship between WSOC, *m/z* 44, and *m/z* 43 provided insight into the contribution of various classes of oxygenated species to WSOC as a result of aerosol aging. The ratio of WSOC : organic was a relatively constant function of *m/z* 44 : 43 during this study, hinting at a greater complexity of WSOC species than explained by either *m/z* 44 or 43. The ratio of *m/z* 44 : WSOC increased as a function of *m/z* 44 : 43 both during the fire- and the non-fire period, suggesting that non-acid oxygenates were being converted to more acidic oxygenates, thereby enhancing the contribution of the latter to WSOC.

This work has illustrated the complexity of factors governing WSOC levels at a fixed point in the Los Angeles Basin. A follow-up study using aircraft observations in the same region during the 2010 CalNex field campaign will extend the discussion of the relative importance of various factors (e.g. transport, meteorology, diverse sources) in governing concentrations and spatiotemporal variability in WSOC in this metropolitan center and outflow regions.

Acknowledgement. This work was supported by the Electric Power Research Institute. The authors gratefully acknowledge the NOAA Air Resources Laboratory (ARL) for provision of the HYSPLIT transport and dispersion model. Analyses and visualizations used in this study were produced with the Giovanni online data system, developed and maintained by the NASA GES DISC. We also acknowledge NASA for the production of the data used in this research effort.

References

Aiken, A. C., Decarlo, P. F., Kroll, J. H., Worsnop, D. R., Huffman, J. A., Docherty, K. S., Ulbrich, I. M., Mohr, C., Kimmel, J. R., Sueper, D., Sun, Y., Zhang, Q., Trimborn, A., Northway, M., Ziemann, P. J., Canagaratna, M. R., Onasch, T. B., Alfarra, M. R., Prevot, A. S. H., Dommen, J., Duplissy, J., Metzger, A., Baltensperger, U., and Jimenez, J. L.: O/C and OM/OC ratios of primary, secondary, and ambient organic aerosols with high-resolution time-of-flight aerosol mass spectrometry, Environ. Sci. Technol., 42, 4478–4485, doi:10.1021/Es703009q, 2008.

Alfarra, M. R., Prevot, A. S. H., Szidat, S., Sandradewi, J., Weimer, S., Lanz, V. A., Schreiber, D., Mohr, M., and Baltensperger, U.: Identification of the mass spectral signature of organic aerosols from wood burning emissions, Environ. Sci. Technol., 41, 5770–5777, doi:10.1021/Es062289b, 2007.

Blumenthal, D. L., White, W. H., and Smith, T. B.: Anatomy of a Los-Angeles smog episode – pollutant transport in daytime sea breeze regime, Atmos. Environ., 12, 893–907, 1978.

Chhabra, P. S., Ng, N. L., Canagaratna, M. R., Corrigan, A. L., Russell, L. M., Worsnop, D. R., Flagan, R. C., and Seinfeld, J. H.: Elemental composition and oxidation of chamber organic aerosol, Atmos. Chem. Phys. Discuss., 11, 10305–10342, doi:10.5194/acpd-11-10305-2011, 2011.

Decesari, S., Fuzzi, S., Facchini, M. C., Mircea, M., Emblico, L., Cavalli, F., Maenhaut, W., Chi, X., Schkolnik, G., Falkovich, A., Rudich, Y., Claeys, M., Pashynska, V., Vas, G., Kourtchev, I., Vermeylen, R., Hoffer, A., Andreae, M. O., Tagliavini, E., Moretti, F., and Artaxo, P.: Characterization of the organic composition of aerosols from Rondônia, Brazil, during the LBA-SMOCC 2002 experiment and its representation through model compounds, Atmos. Chem. Phys., 6, 375–402, doi:10.5194/acp-6-375-2006, 2006.

Docherty, K. S., Stone, E. A., Ulbrich, I. M., DeCarlo, P. F., Snyder, D. C., Schauer, J. J., Peltier, R. E., Weber, R. J., Murphy, S. M., Seinfeld, J. H., Eatough, D. J., Grover, B. D., and Jimenez, J. L.: Apportionment of primary and secondary organic aerosols in Southern California during the 2005 study of organic aerosols in riverside (SOAR), Environ. Sci. Technol., 42, 7655–7662, 2008.

Draxler, R. R. and Rolph, G. D.: HYSPLIT (HYbrid Single-Particle Lagrangian Integrated Trajectory) Model access via NOAA ARL READY Website, available at: http://www.arl.noaa.gov/ready/hysplit4.html, NOAA Air Resources Laboratory, Silver Spring (last access: August 2010), 2003.

Drewnick, F., Hings, S. S., DeCarlo, P., Jayne, J. T., Gonin, M., Fuhrer, K., Weimer, S., Jimenez, J. L., Demerjian, K. L., Borrmann, S., and Worsnop, D. R.: A new time-of-flight aerosol mass spectrometer (TOF-AMS) – Instrument description and first field deployment, Aerosol Sci. Tech., 39, 637–658, doi:10.1080/027868290500182040, 2005.

Ervens, B. and Volkamer, R.: Glyoxal processing by aerosol multiphase chemistry: towards a kinetic modeling framework of secondary organic aerosol formation in aqueous particles, Atmos. Chem. Phys., 10, 8219–8244, doi:10.5194/acp-10-8219-2010, 2010.

Fuzzi, S., Decesari, S., Facchini, M. C., Cavalli, F., Emblico, L., Mircea, M., Andreae, M. O., Trebs, I., Hoffer, A., Guyon, P., Artaxo, P., Rizzo, L. V., Lara, L. L., Pauliquevis, T., Maenhaut, W., Raes, N., Chi, X. G., Mayol-Bracero, O. L., Soto-Garcia, L. L., Claeys, M., Kourtchev, I., Rissler, J., Swietlicki, E., Tagliavini, E., Schkolnik, G., Falkovich, A. H., Rudich, Y., Fisch, G., and Gatti, L. V.: Overview of the inorganic and organic composition of size-segregated aerosol in Rondonia, Brazil, from the biomass-burning period to the onset of the wet season, J. Geophys. Res., 112, D01201, doi:10.1029/2005jd006741, 2007.

Gao, S., Hegg, D. A., Hobbs, P. V., Kirchstetter, T. W., Magi, B. I., and Sadilek, M.: Water-soluble organic components in aerosols associated with savanna fires in Southern Africa: identification, evolution, and distribution, J. Geophys. Res., 108, 8491, doi:10.1029/2002JD002324, 2003.

Graham, B., Mayol-Bracero, O. L., Guyon, P., Roberts, G. C., Decesari, S., Facchini, M. C., Artaxo, P., Maenhaut, W., Koll, P., and Andreae, M. O.: Water-soluble organic compounds in biomass burning aerosols over Amazonia – 1. Characterization by NMR and GC-MS, J. Geophys. Res., 107, 8047, doi:10.1029/2001jd000336, 2002.

Grieshop, A. P., Logue, J. M., Donahue, N. M., and Robinson, A. L.: Laboratory investigation of photochemical oxidation of organic aerosol from wood fires 1: measurement and simulation of organic aerosol evolution, Atmos. Chem. Phys., 9, 1263–1277, doi:10.5194/acp-9-1263-2009, 2009.

Hennigan, C. J., Bergin, M. H., Dibb, J. E., and Weber, R. J.: Enhanced secondary organic aerosol formation due to water uptake by fine particles, Geophys. Res. Lett., 35, L18801, doi:10.1029/2008gl035046, 2008.

Hennigan, C. J., Bergin, M. H., Russell, A. G., Nenes, A., and Weber, R. J.: Gas/particle partitioning of water-soluble organic aerosol in Atlanta, Atmos. Chem. Phys., 9, 3613–3628, doi:10.5194/acp-9-3613-2009, 2009.

Hennigan, C. J., Sullivan, A. P., Collett Jr., J. L., and Robinson, A. L.: Levoglucosan stability in biomass burning particles exposed to hydroxyl radicals, Geophys. Res. Lett., 37, L09806, doi:10.1029/2010GL043088, 2010.

Hersey, S. P., Craven, J. S., Schilling, K. A., Metcalf, A. R., Sorooshian, A., Chan, M. N., Flagan, R. C., and Seinfeld, J. H.: The Pasadena Aerosol Characterization Observatory (PACO): chemical and physical analysis of the Western Los Angeles Basin aerosol, Atmos. Chem. Phys. Discuss., 11, 5867–5933, doi:10.5194/acpd-11-5867-2011, 2011.

Hughes, L. S., Allen, J. O., Salmon, L. G., Mayo, P. R., Johnson, R. J., and Cass, G. R.: Evolution of nitrogen species air pollutants along trajectories crossing the Los Angeles area,

Environ. Sci. Technol., 36, 3928–3935, 2002.
Husar, R. B., Patterson, D. E., Blumenthal, D. L., White, W. H., and Smith, T. B.: 3-dimensional distribution of air-pollutants in Los-Angeles Basin, J. Appl. Meteorol., 16, 1089–1096, 1977.
Jaffrezo, J.-L., Aymoz, G., Delaval, C., and Cozic, J.: Seasonal variations of the water soluble organic carbon mass fraction of aerosol in two valleys of the French Alps, Atmos. Chem. Phys., 5, 2809–2821, doi:10.5194/acp-5-2809-2005, 2005.
Kondo, Y., Miyazaki, Y., Takegawa, N., Miyakawa, T., Weber, R. J., Jimenez, J. L., Zhang, Q., and Worsnop, D. R.: Oxygenated and water-soluble organic aerosols in Tokyo, J. Geophys. Res., D01203, doi:10.1029/2006jd007056, 2007.
Lee, S., Kim, H. K., Yan, B., Cobb, C. E., Hennigan, C., Nichols, S., Chamber, M., Edgerton, E. S., Jansen, J. J., Hu, Y. T., Zheng, M., Weber, R. J., and Russell, A. G.: Diagnosis of aged prescribed burning plumes impacting an urban area, Environ. Sci. Technol., 42, 1438–1444, doi:10.1021/Es7023059, 2008.
Lu, R., and Turco, R. P.: Air pollutant transport in a coastal environment. 2. 3-Dimensional simulations over Los-Angeles Basin, Atmos. Environ., 29, 1499–1518, 1995.
Mayol-Bracero, O. L., Guyon, P., Graham, B., Roberts, G., Andreae, M. O., Decesari, S., Facchini, M. C., Fuzzi, S., and Artaxo, P.: Water-soluble organic compounds in biomass burning aerosols over Amazonia – 2. Apportionment of the chemical composition and importance of the polyacidic fraction, J. Geophys. Res., 107, 8091, doi:10.1029/2001jd000522, 2002.
McLafferty, F. W. and Turecek, F.: Interpretation of Mass Spectra, 4th Edn., University Science Books, Mill Valley, California, 1993.
Miyazaki, Y., Kondo, Y., Takegawa, N., Komazaki, Y., Fukuda, M., Kawamura, K., Mochida, M., Okuzawa, K., and Weber, R. J.: Time-resolved measurements of water-soluble organic carbon in Tokyo, J. Geophys. Res., 111, D23206, doi:10.1029/2006jd007125, 2006.
Murphy, S. M., Agrawal, H., Sorooshian, A., Padro, L. T., Gates, H., Hersey, S., Welch, W. A., Jung, H., Miller, J. W., Cocker, D. R., Nenes, A., Jonsson, H. H., Flagan, R. C., and Seinfeld, J. H.: Comprehensive simultaneous shipboard and airborne characterization of exhaust from a modern container ship at sea, Environ. Sci. Technol., 43, 4626–4640, doi:10.1021/Es802413j, 2009.
Ng, N. L., Canagaratna, M. R., Zhang, Q., Jimenez, J. L., Tian, J., Ulbrich, I. M., Kroll, J. H., Docherty, K. S., Chhabra, P. S., Bahreini, R., Murphy, S. M., Seinfeld, J. H., Hildebrandt, L., Donahue, N. M., DeCarlo, P. F., Lanz, V. A., Prévôt, A. S. H., Dinar, E., Rudich, Y., and Worsnop, D. R.: Organic aerosol components observed in Northern Hemispheric datasets

from Aerosol Mass Spectrometry, Atmos. Chem. Phys., 10, 4625–4641, doi:10.5194/acp-10-4625-2010, 2010.

Peltier, R. E., Weber, R. J., and Sullivan, A. P.: Investigating a liquid-based method for online organic carbon detection in atmospheric particles, Aerosol Sci. Tech., 41, 1117–1127, doi:10.1080/02786820701777465, 2007.

Phuleria, H. C., Fine, P. M., Zhu, Y. F., and Sioutas, C.: Air quality impacts of the October 2003 Southern California wildfires, J. Geophys. Res., 110, D07S20, doi:10.1029/2004jd004626, 2005.

Posfai, M., Simonics, R., Li, J., Hobbs, P. V., and Buseck, P. R.: Individual aerosol particles from biomass burning in Southern Africa: 1. Composition and size distributions of carbonaceous particles, J. Geophys. Res., 108(D13), 8483, doi:10.1029/2002JD002291, 2003.

Reid, J. S., Koppmann, R., Eck, T. F., and Eleuterio, D. P.: A review of biomass burning emissions part II: intensive physical properties of biomass burning particles, Atmos. Chem. Phys., 5, 799–825, doi:10.5194/acp-5-799-2005, 2005.

Robinson, A. L., Donahue, N. M., Shrivastava, M. K., Weitkamp, E. A., Sage, A. M., Grieshop, A. P., Lane, T. E., Pierce, J. R., and Pandis, S. N.: Rethinking organic aerosols: semivolatile emissions and photochemical aging, Science, 315, 1259–1262, doi:10.1126/science.1133061, 2007.

Ruellan, S., Cachier, H., Gaudichet, A., Masclet, P., and Lacaux, J. P.: Airborne aerosols over Central Africa during the experiment for regional sources and sinks of oxidants (EXPRESSO), J. Geophys. Res., 104, 30673–30690, 1999.

Sorooshian, A., Brechtel, F. J., Ma, Y. L., Weber, R. J., Corless, A., Flagan, R. C., and Seinfeld, J. H.: Modeling and characterization of a particle-into-liquid sampler (PILS), Aerosol Sci. Tech., 40, 396–409, doi:10.1080/02786820600632282, 2006.

Sorooshian, A., Murphy, S. M., Hersey, S., Bahreini, R., Jonsson, H., Flagan, R. C., and Seinfeld, J. H.: Constraining the contribution of organic acids and AMS *m/z* 44 to the organic aerosol budget: on the importance of meteorology, aerosol hygroscopicity, and region, Geophys. Res. Lett., 37, L21807, doi:10.1029/2010GL044951, 2010.

Sullivan, A. P. and Weber, R. J.: Chemical characterization of the ambient organic aerosol soluble in water: 1. Isolation of hydrophobic and hydrophilic fractions with a XAD-8 resin, J. Geophys. Res., 111, D05314, doi:10.1029/2005jd006485, 2006.

Sullivan, A. P., Weber, R. J., Clements, A. L., Turner, J. R., Bae, M. S., and Schauer, J. J.: A method for on-line measurement of water-soluble organic carbon in ambient aerosol particles: results from an urban site, Geophys. Res. Lett., 31, L13105, doi:10.1029/2004gl019681, 2004.

Sullivan, A. P., Peltier, R. E., Brock, C. A., de Gouw, J. A., Holloway, J. S., Warneke, C., Wollny, A. G., and Weber, R. J.: Airborne measurements of carbonaceous aerosol soluble in water over Northeastern United States: method development and an investigation into water-soluble organic carbon sources, J. Geophys. Res., 111, D23S46, doi:10.1029/2006jd007072, 2006.

Timonen, H., Aurela, M., Carbone, S., Saarnio, K., Saarikoski, S., Mäkelä, T., Kulmala, M., Kerminen, V. M., Worsnop, D. R., and Hillamo, R.: High time-resolution chemical characterization of the water-soluble fraction of ambient aerosols with PILS-TOC-IC and AMS, Atmos. Meas. Tech., 3, 1063–1074, doi:10.5194/amt-3-1063-2010, 2010.

Vutukuru, S., Griffin, R. J., and Dabdub, D.: Simulation and analysis of secondary organic aerosol dynamics in the South Coast Air Basin of California, J. Geophys. Res., 111, D10S12, doi:10.1029/2005jd006139, 2006.

Weber, R. J., Sullivan, A. P., Peltier, R. E., Russell, A., Yan, B., Zheng, M., de Gouw, J., Warneke, C., Brock, C., Holloway, J. S., Atlas, E. L., and Edgerton, E.: A study of secondary organic aerosol formation in the anthropogenic-influenced Southeastern United States, J. Geophys. Res., 112, D13302, doi:10.1029/2007jd008408, 2007.

Westerling, A. L., Hidalgo, H. G., Cayan, D. R., and Swetnam, T. W.: Warming and earlier spring increase Western US forest wildfire activity, Science, 313, 940–943, doi:10.1126/science.1128834, 2006.

Zhang, Q., Alfarra, M. R., Worsnop, D. R., Allan, J. D., Coe, H., Canagaratna, M. R., and Jimenez, J. L.: Deconvolution and quantification of hydrocarbon-like and oxygenated organic aerosols based on aerosol mass spectrometry, Environ. Sci. Technol., 39, 4938–4952, doi:10.1021/Es048568l, 2005.

Table 1. Statistical summary of the relationship between WSOC (μg C m^{-3}) and other chemical and meteorological parameters (measured at Santa Fe Dam). AMS aerosol species concentration units are μg m^{-3}.

		Station fire				No fire			
		r^2	Slope	Intercept	*n*	r^2	Slope	Intercept	*n*
AMS	Total organic	0.92	−1.05	0.34	1298	0.47	0.14	0.69	1557
(μg m^{-3})	*m/z* 60	0.90	40.16	1.88	1298	0.45	94.46	0.48	1557
	m/z 44	0.84	3.04	−1.15	1298	0.35	0.95	0.94	1557
	m/z 43	0.84	5.22	−1.45	1298	0.49	2.25	0.51	1557
	m/z 55	0.80	9.47	−1.43	1298	0.45	3.79	0.61	1557
	NO_3^-	0.79	4.30	−1.09	1298	0.00	−0.02	1.75	1557
	Cl^-	0.57	77.39	0.99	1296	0.03	−1.28	1.82	1557
	m/z 57	0.47	1.24	0.60	1298	0.20	6.58	0.96	1557
	NH_4^+	0.18	7.06	0.54	1298	0.00	0.04	1.64	1557
	SO_4^{2-}	0.14	−2.67	7.41	1298	0.08	0.14	1.40	1557
Gas	CO (ppm$_v$)	0.18	3.66	2.78	151	0.00	0.26	1.69	212
	O_3 (ppb$_v$)	0.05	0.03	3.35	151	0.35	0.02	0.83	212
	NO_x (ppb$_v$)	−0.01	−0.01	4.77	151	0.03	−0.01	1.94	212
Meteorology	Wind speed (m s^{-1})	0.07	–	–	144	0.11	–	–	210
	Solar radiation (W m^{-2})	0.00	–	–	148	0.28	–	–	209
	T (°C)	0.01	–	–	144	0.44	–	–	209
	RH (%)	0.00	–	–	147	0.14	–	–	209

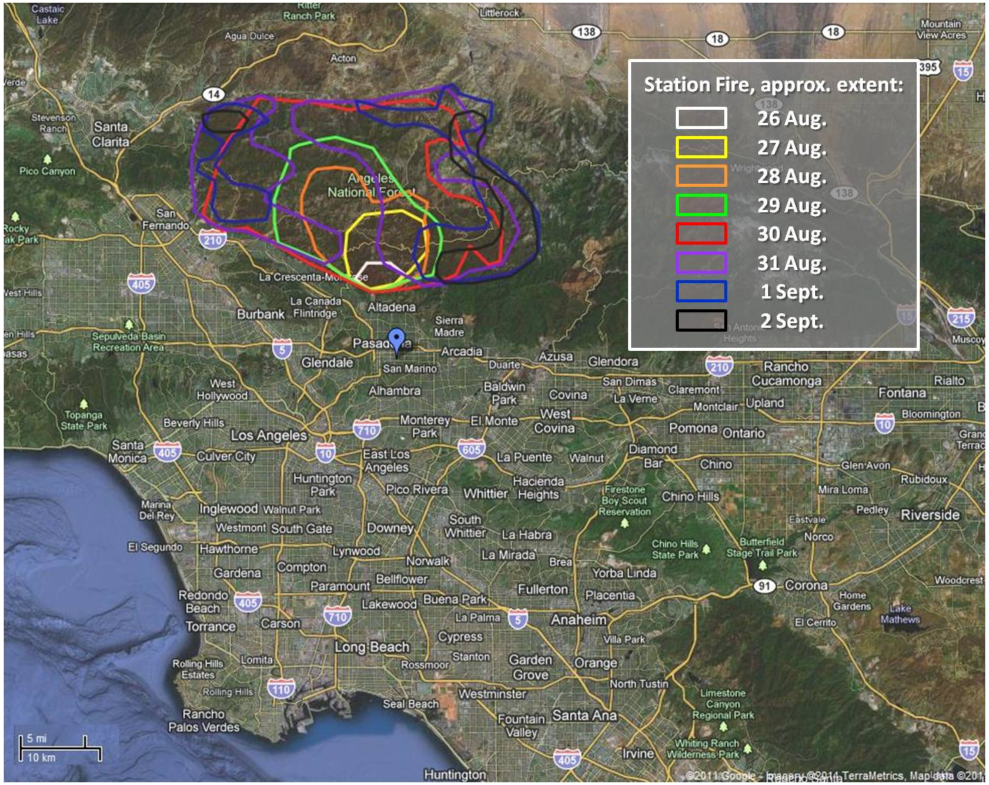

Fig. 1. Approximate spatial extent of the Station Fire by date (bordered areas). The fire area was estimated using fire maps by "Firefly", University of Maryland (http://firefly.geog.umd.edu/firemap/). The blue marker in Pasadena represents the measurement site.

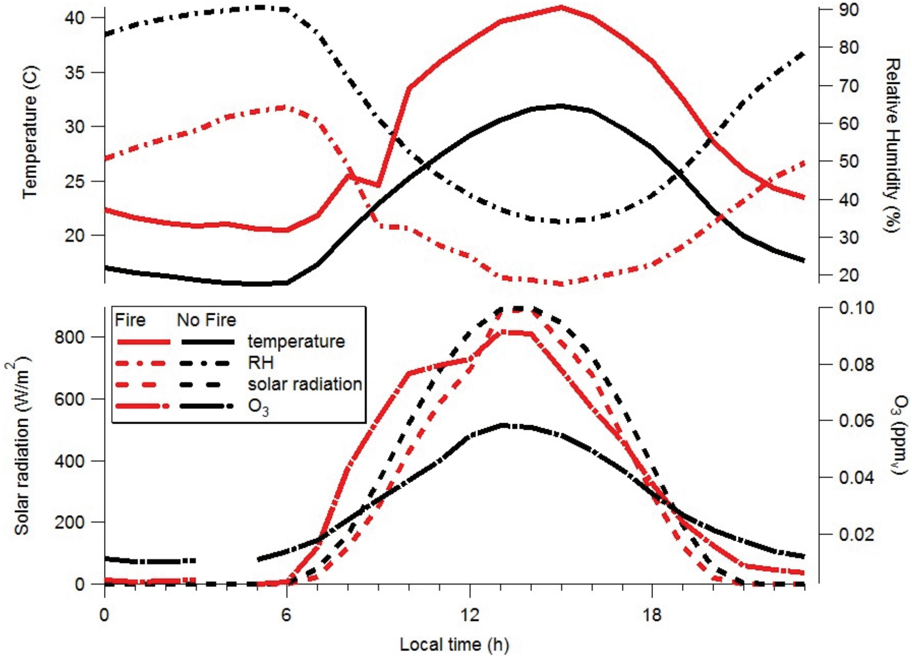

Fig. 2. Diurnal meteorological parameters (Santa Fe Dam station) and O_3 concentrations.

Title Page
Abstract | Introduction
Conclusions | References
Tables | Figures
◀| |▶
◀ ▶
Back | Close
Full Screen / Esc
Printer-friendly Version
Interactive Discussion

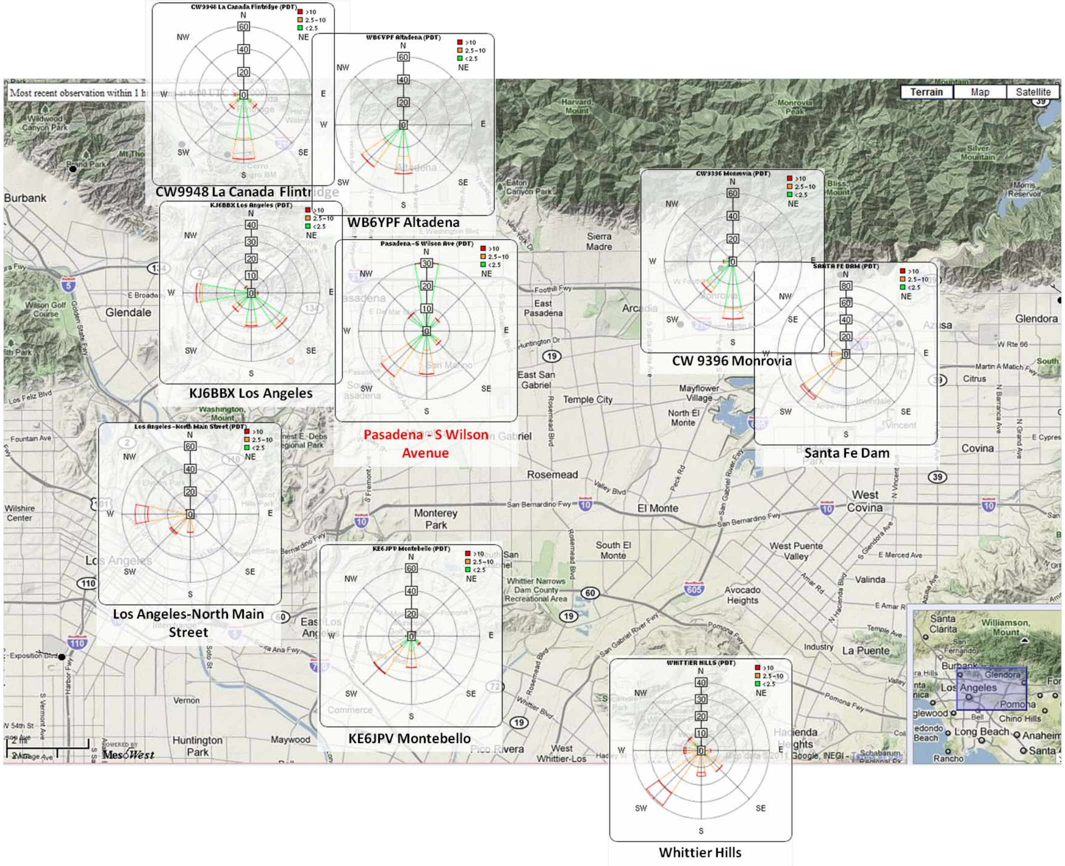

Fig. 3. Wind roses for the month of July for South Wilson Avenue and surrounding stations (data from Mesowest, http://mesowest.utah.edu/index.html).

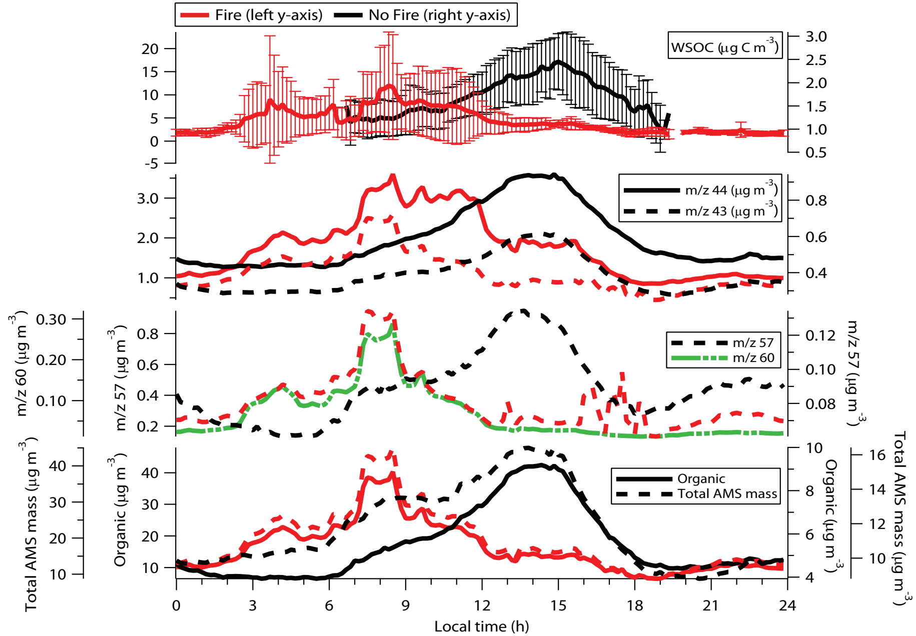

Fig. 4. Diurnal averages of aerosol chemistry (*m/z* 60 shown for the fire period only).

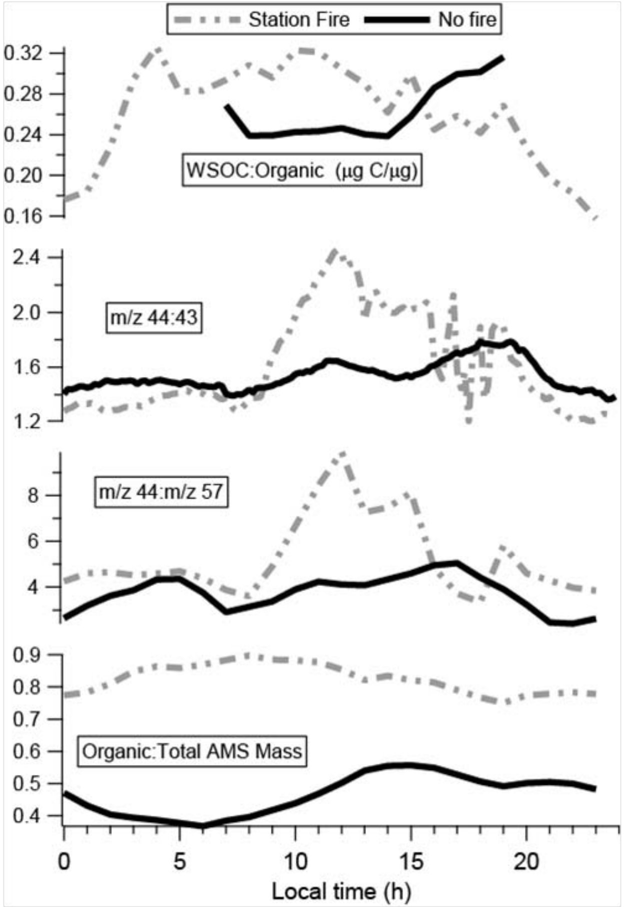

Fig. 5. Diurnally averaged ratios of different aerosol measurements.

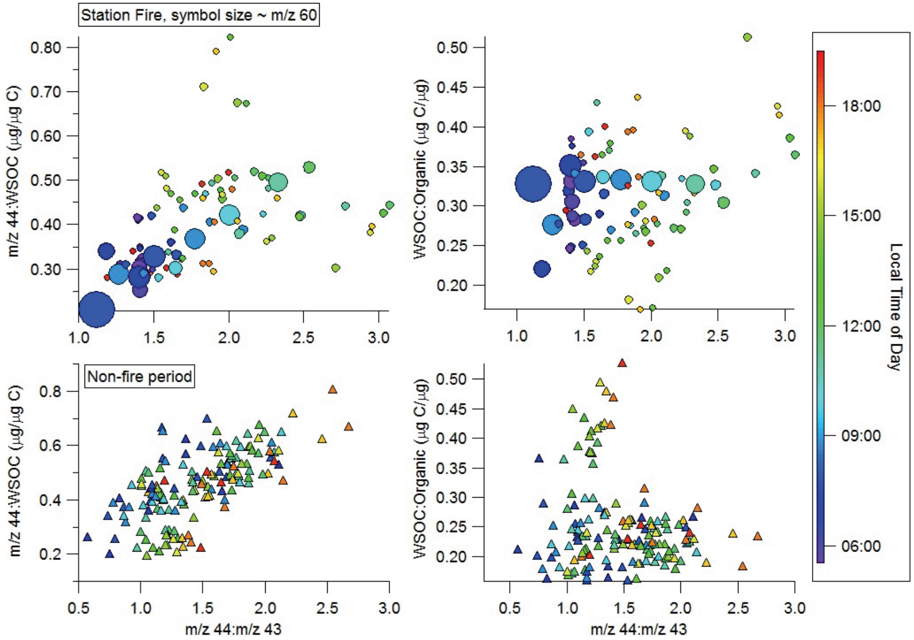

Fig. 6. Summary of the ratios WSOC : organic and *m/z* 44 : WSOC as functions of *m/z* 44 : 43 during the (top panels) fire and (bottom panels) the non-fire periods. Symbols are color-coded by time of day, and in the fire panels the symbol sizes are proportional to the tracer for biomass burning *m/z* 60 (range = 0.03–0.9 µg m^{-3}).

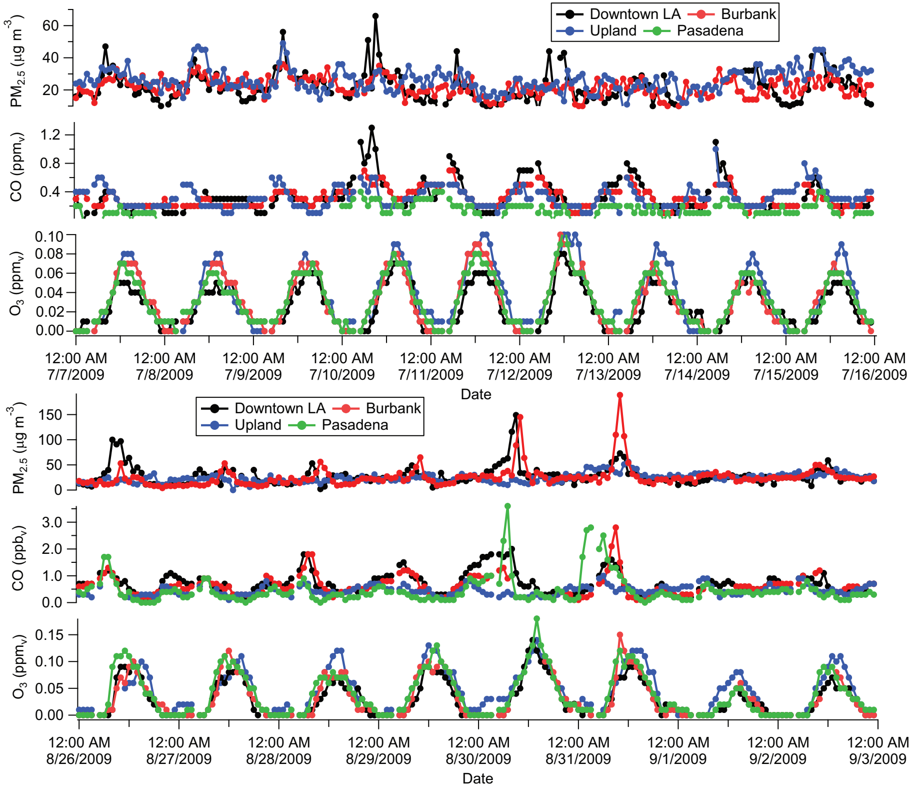

Fig. 7. Ground station observations of PM$_{2.5}$, CO and O$_3$ for the non-fire (top) and the fire (bottom) period. The four stations (http://www.arb.ca.gov) are shown on the map in Fig. 1.

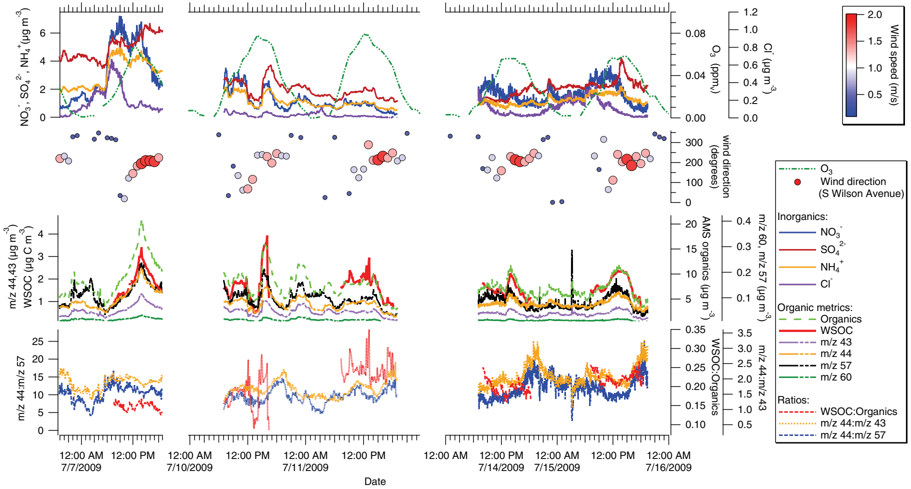

Fig. 8. Time series of various measured and derived parameters during selected days outside the fire period. The symbol size for wind direction is proportional to measured wind speed.

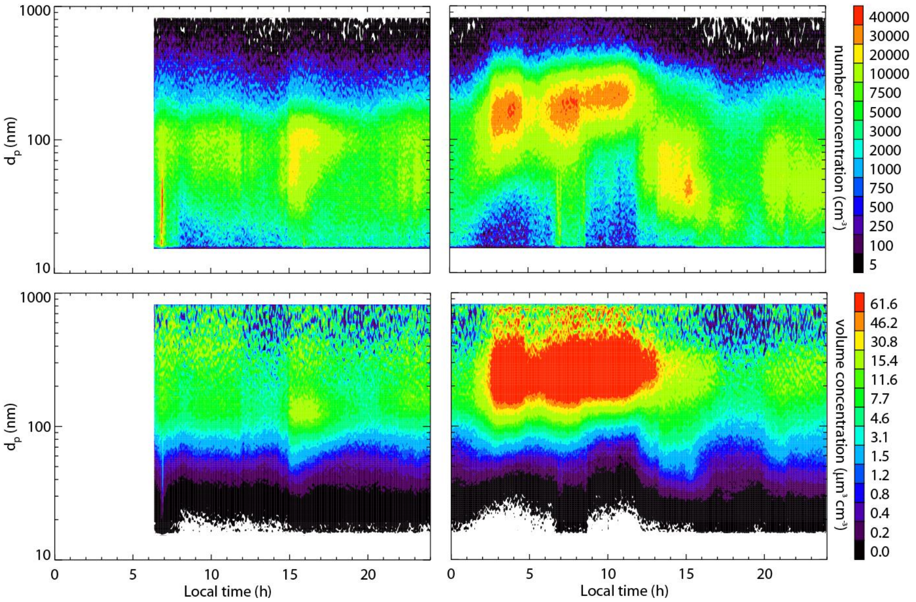

Fig. 9. Number (top) and volume (bottom) size distributions over the course of (left) 10 July 2009, a day of the non-fire period, and (right) 31 August 2009 in the fire period.

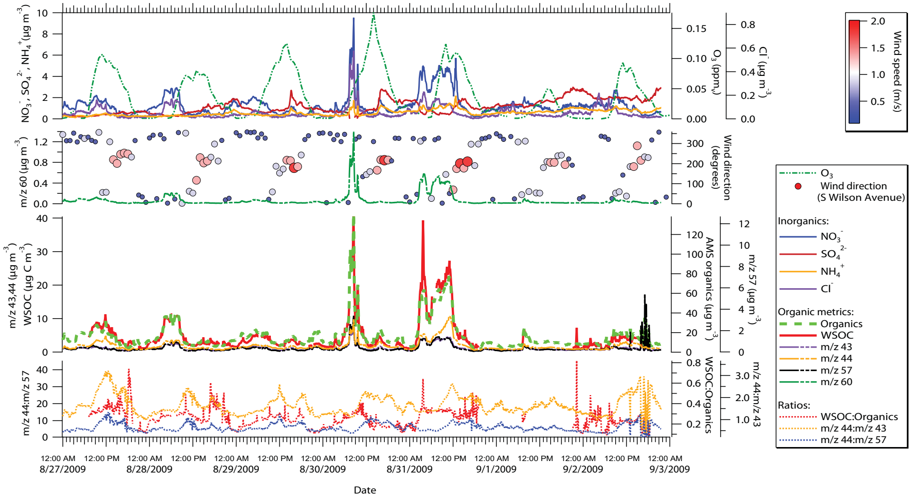

Fig. 10. Time series of various measured and derived parameters during the fire period. The symbol size for wind direction is proportional to measured wind speed.